Proceedings of SMASIS08
ASME Conference on Smart Materials, Adaptive Structures and Intelligent Systems
October 28-30, 2008, Ellicott City, Maryland, USA

SMASIS2008-328

FULLY-COUPLED MODEL FOR 3-D INDUCTION AND STRAIN OF GALFENOL WITH GEOMETRY EFFECTS AND APPLIED CURRENTS

Phillip Evans
Department of Mechanical Engineering
The Ohio State University
Columbus, Ohio 43210
Email: evans.895@osu.edu

Marcelo Dapino*
Department Mechanical Engineering
The Ohio State University
Columbus, Ohio, 43210
Email: dapino.1@osu.edu

ABSTRACT

A fully-coupled and 3-D model for induction and strain of cubic magnetostrictive materials is presented which incorporates geometry dependent demagnetizing fields, current induced fields, and stress dependent permeability. Maxwell's equations are coupled with a nonlinear constitutive model derived through thermodynamics. Discretization of the nonlinear problem with a known reference configuration yields a piecewise linear model ideal for transducer design.

NOMENCLATURE

$\mathbf{A}$ Magnetic potential
$\mathbf{B}$ Magnetic induction
$b_{1,2}$ Magnetoelastic coupling coefficients
$\mathbf{c}$ Stiffness matrix
$\mathbf{d}_1$ Linear stress-induction matrix
$\mathbf{d}_2$ Linear strain-field matrix
$\mathbf{F}$ Body force
$\mathbf{H}$ Magnetic field
K_4 Fourth-order anisotropy constant
K_p Domain pinning constant
$\mathbf{M}$ Magnetization
$\mathbf{m}$ Magnetic domain orientation
M_s Saturation magnetization
$\mathbf{S}$ Total strain
$\mathbf{S}_e$ Elastic strain
$\mathbf{S}_{me}$ Magnetoelastic strain
$\mathbf{T}$ Stress
$\mathbf{u}$ Displacement
$\lambda_{100,111}$ Magnetostriction coefficients
η Entropy
θ Temperature
ξ Domain family volume fraction

INTRODUCTION

Magnetostrictive materials exhibit coupling between magnetic and mechanical states. Galfenol (Fe_xGa_{1-x}, $13 \leq x \leq 29$ at%) is a new magnetostrictive material which exhibits moderate magnetostriction (strain due to magnetoelastic coupling) and steel-like structural properties [1]. Its mechanical properties allow it to be machined, rolled, deposited, and welded. Galfenol is capable of bearing compressive, tensile, bending, torsion, and shock loads. This unique combination of robust mechanical properties and moderate magnetostriction makes Galfenol well suited for creating adaptive, load-bearing structures with complex geometries. This has motivated the development of 3-D magnetomechanical models [2–4]. The existing models are typically implemented with the finite element method and consist of a set of Maxwell's equations coupled to the law of conservation of momentum through a material constitutive law. An efficient and accurate framework is desirable for use as a tool for design and control of Galfenol devices that can be utilized in the full nonlinear regime.

Oates [2] extended the 1-D homogenized energy framework of Smith et al. [5] to 3-D by including the effect of multi-axial magnetic moment switching in the macroscopic magnetization. Demagnetizing fields dependent on transducer geometry are accounted for by coupling the constitutive model with Gauss' law. The framework is implemented with negligible magnetoelastic coupling and in the absence of applied currents. Mudivarthi et al. [3] include magnetoelastic coupling with no current densities by using the magnetomechanical constitutive model of Armstrong [6] to couple Gauss' law with the law of conservation of momentum where Gauss law accounts for the geometry dependent demagnetizing fields and the coupling with momentum conservation accounts for stress dependent magnetization changes. Kiefer et al. [4] include Ampère's law with Gauss' law and momentum conservation. A nonlinear numerical solution technique using the finite element method and Newton-Raphson iteration is

*Address all correspondence to this author.

developed. The framework is implemented with a linear constitutive law in the absence of current densities.

This work develops a magnetomechanical modeling framework which includes current density induced magnetic fields through Ampère's law, demagnetizing fields from Gauss' law, and magnetomechanical coupling. A computationally efficient and nonlinear constitutive model is used to couple the Ampère and Gauss laws with momentum conservation. Piecewise linearization of the constitutive model starting from a known configuration over the boundary value problem is used to avoid iteration which is necessary when solving nonlinear problems.

MAGNETIC BOUNDARY VALUE PROBLEM

When motion and applied currents are quasi-static, Maxwell's electromagnetic equations reduce to the two laws of magnetostatics

$$\nabla \cdot \mathbf{B} = 0, \tag{1}$$
$$\nabla \times \mathbf{H} = \mathbf{J}. \tag{2}$$

Gauss' law (1) accounts for demagnetizing fields and Ampère's law (2) accounts for current-induced magnetic fields. The vector magnetic potential is introduced with $\mathbf{B} = \nabla \times \mathbf{A}$ in order to identically satisfy (1). To solve the magnetic problem, a constitutive relation $\mathbf{B} = \mu_0 \left[\mathbf{H} + \mathbf{M}\left(\mathbf{H}, \mathbf{T}\right)\right]$ is needed to reformulate (2) in terms of the vector magnetic potential; the stress dependence is a result of the intrinsic magnetomechanical coupling present in magnetostrictive materials. A typical problem geometry consists of a magnetic material surrounded by an air volume which is sufficiently large so that $\mathbf{A} = 0$ on the boundary. Additionally, a conductor with current density generates a magnetic field.

MECHANICAL BOUNDARY VALUE PROBLEM

Force balance dictates that the body force be balanced by the divergence of the stress

$$\mathbf{F} = -\nabla \cdot \mathbf{T}. \tag{3}$$

Since the boundary often consists of fixed or free conditions for displacement, the mechanical boundary value problem is typically reformulated in terms of displacements; this is done by relating stress to strain and strain to displacement. For linear elastic materials under the small displacement assumption, the total strain is the sum of the elastic strain and the magnetoelastic strain: $\mathbf{S} = \mathbf{S}_e + \mathbf{S}_{me}(\mathbf{H}, \mathbf{T})$, the elastic strain is given by Hooke's law $\mathbf{S}_e = \mathbf{c}^{-1}\mathbf{T}$, and the displacement is related to the strain by $\mathbf{S} = \nabla \mathbf{u}$. The form of stiffness tensor $\mathbf{c}$ depends on the material symmetry. The stress and field dependence in the magnetoelastic strain or magnetostriction and in the magnetic induction couple the magnetic and mechanical boundary value problems.

CONSTITUTIVE MODEL

A constitutive model relating stress and magnetic field to magnetic induction and strain is needed to solve the coupled magnetic and mechanical boundary value problem. Ferromagnetic materials consist of regions of uniform magnetization or domains. For cubic materials with a positive fourth-order anisotropy constant, there are six possible domain orientations for thermodynamic equilibrium to be achieved. These orientations are near the $\langle 100 \rangle$ crystal directions and depend on stress and magnetic field. The macroscopic magnetization and magnetostriction are the sum of the contributions of the six domain families

$$(\mathbf{M}, \mathbf{S}_{me}) = \sum_{k=1}^{6} \left(\mathbf{M}^k, \mathbf{S}_{me}^k\right) \xi^k. \tag{4}$$

The stress and field dependent magnetization and magnetostriction of each domain family can be found from the Gibbs free energy of a domain. This is obtained by subtracting the magnetoelastic and mechanical work energies from the internal energy. For cubic magnetostrictive materials the energy is

$$\begin{aligned} G(\mathbf{H}, \mathbf{T}) = &K_4 \left(m_1 m_2 + m_2 m_3 + m_3 m_1\right) \\ &- \mathbf{S}_{me} \cdot \mathbf{T} - \mu_0 \mathbf{M} \cdot \mathbf{H}, \end{aligned} \tag{5}$$

where $\mathbf{M} = M_s \begin{bmatrix} m_1 & m_2 & m_3 \end{bmatrix}$. The first term is the internal energy due to magnetocrystalline anisotropy which for $K_4 > 0$ is minimum in the six $\langle 100 \rangle$ directions. Rotation away from these directions requires work from applied stress or field which is accounted for in the second two energy terms. The dependent variable is magnetic domain orientation and independent variables are stress and field. The magnetostriction is only a function of stress and field through its dependence on $\mathbf{m}$ which for the longitudinal components is

$$S_{me,i} = \frac{3}{2}\lambda_{100} m_i^2, \quad i = 1, 2, 3 \tag{6}$$

and shear components

$$\begin{aligned} S_{me,4} &= 3\lambda_{111} m_1 m_2, \\ S_{me,5} &= 3\lambda_{111} m_2 m_3, \\ S_{me,6} &= 3\lambda_{111} m_3 m_1. \end{aligned} \tag{7}$$

A derivation of these expressions from energy principles has been given by Kittel [7]. The six equilibrium domain orientations are calculated from $\partial G / \partial \mathbf{m} = 0$.

The stress and field dependent domain volume fractions can be found from the Gibbs energy of a collection of domains which includes an ordering term due to entropy

$$\bar{G} = -\eta\theta + \sum_{k=1}^{6} \xi^k G^k, \tag{8}$$

where G^k is the Gibbs free energy of the k^{th} equilibrium domain orientation. The entropy of a system having six possible energy states can be formulated from statistical mechanics [8] and is

$$\eta = -\frac{k_B}{V}\sum_{k=1}^{6}\xi^k \ln \xi^k. \tag{9}$$

The equilibrium domain configuration ξ^k is obtained from the equilibrium conditions $\partial\bar{G}/\partial\xi^k = 0$, constrained to $\sum_{k=1}^{6}\xi^k = 1$, which yields

$$\xi^k = \frac{e^{-G^k V/k_B\theta}}{\sum_{j=1}^{6} e^{-G^j V/k_B\theta}}. \tag{10}$$

Expressions (6), (7) and (10), along with the six equilibrium domain orientations $\mathbf{m}^k$ calculated from the domain level Gibbs free energy are substituted into (4) to yield the macroscopic magnetization and magnetostriction.

The stress and field dependence of the macroscopic magnetization and magnetostriction as given by (4) is shown in Figure 1. Smooth and nonlinear constitutive behavior is achieved without using homogenization techniques which involve integration; this computational efficiency is advantageous for the finite element solution of the magnetic and mechanical boundary value problems where the constitutive model is evaluated at each node.

Hysteresis can be incorporated into the constitutive behavior by accounting for the delay in domain volume fraction change due to domain wall pinning; domain wall motion is a mechanism for volume fraction changes. According to Armstrong [9] the evolution of volume fractions in the presence of domain wall pinning is

$$\frac{d\xi^k}{dH} = (\xi^k_{\text{an}} - \xi^k)/K_p, \tag{11}$$

where ξ^k_{an} is the anhysteretic volume fraction from (10).

PIECE-WISE LINEAR MODEL

From (4) the stress and field dependent differentials $\partial\mathbf{B}/\partial\mathbf{H} = \boldsymbol{\mu}$, $\partial\mathbf{B}/\partial\mathbf{T} = \mathbf{d}_1$, and $\partial\mathbf{S}/\partial\mathbf{H} = \mathbf{d}_2$ can be calculated. For small changes in the stress $\tilde{\mathbf{T}} = \mathbf{T} - \mathbf{T}_0$ and field $\tilde{\mathbf{H}} = \mathbf{H} - \mathbf{H}_0$, the induction and strain are then given by

$$\begin{aligned}\mathbf{B} &= \mathbf{B}_0 + \boldsymbol{\mu}(\mathbf{H}_0,\mathbf{T}_0)\tilde{\mathbf{H}} + \mathbf{d}_1(\mathbf{H}_0,\mathbf{T}_0)\tilde{\mathbf{T}},\\ \mathbf{S} &= \mathbf{S}_0 + \mathbf{c}^{-1}\tilde{\mathbf{T}} + \mathbf{d}_2(\mathbf{H}_0,\mathbf{T}_0)\tilde{\mathbf{H}}.\end{aligned} \tag{12}$$

Defining the quantities $\tilde{\mathbf{B}} = \mathbf{B} - \mathbf{B}_0$, $\tilde{\mathbf{S}} = \mathbf{S} - \mathbf{S}_0$, $\tilde{\mathbf{A}} = \mathbf{A} - \mathbf{a}_0$, $\tilde{\mathbf{u}} = \mathbf{u} - \mathbf{u}_0$, $\tilde{\mathbf{F}} = \mathbf{F} - \mathbf{F}_0$, and $\tilde{\mathbf{J}} = \mathbf{J} - \mathbf{J}_0$, the following relations hold since all operators involved are linear

$$\tilde{\mathbf{B}} = \nabla \times \tilde{\mathbf{A}}, \tag{13}$$

$$\nabla \times \tilde{\mathbf{H}} = \tilde{\mathbf{J}}, \tag{14}$$

$$-\nabla \cdot \tilde{\mathbf{T}} = \tilde{\mathbf{F}}, \tag{15}$$

$$\tilde{\mathbf{S}} = \nabla\tilde{\mathbf{u}}. \tag{16}$$

The constitutive equations (12) and relations (13)- (16) can be combined into the linear, coupled boundary value problem

$$\begin{aligned}\nabla \times \left(\mathcal{C}^M \nabla \times \tilde{\mathbf{A}}\right) + \nabla \times \left(\mathcal{C}^{ME}_M \nabla\tilde{\mathbf{u}}\right) &= \tilde{\mathbf{J}},\\ -\nabla \cdot \left(\mathcal{C}^E \nabla\tilde{\mathbf{u}}\right) - \nabla \cdot \left(\mathcal{C}^{ME}_E \nabla \times \tilde{\mathbf{A}}\right) &= \tilde{\mathbf{F}}.\end{aligned} \tag{17}$$

The coefficient matrices $\mathcal{C}$ are functions of the initial magnetic field and stress. In the absence of magnetomechanical coupling,

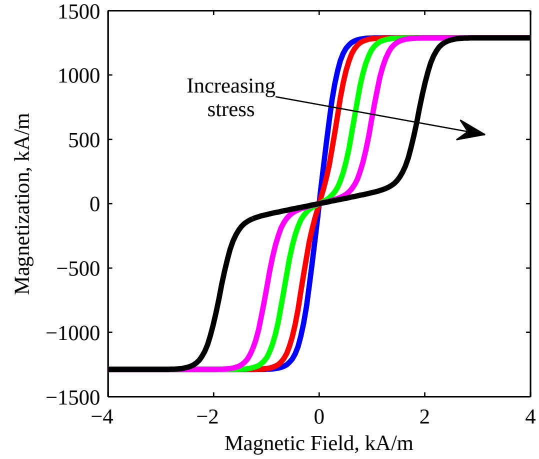

(a)

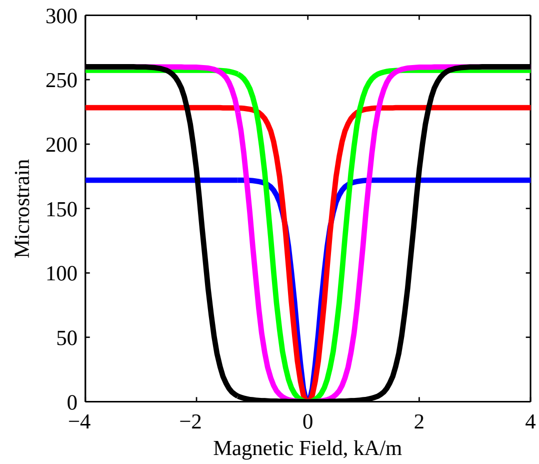

(b)

Figure 1. SIMULATED (a) MAGNETIZATION AND (b) MAGNETOELASTIC STRAIN RESPONSE TO MAGNETIC FIELD AND BIAS STRESS OF 0, -5, -15,-25, and -40 MPa.

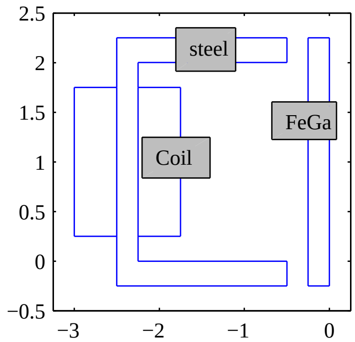

Figure 2. GEOMETRY OF BOUNDARY VALUE PROBLEM.

$\mathcal{C}^M$ reduces to $\boldsymbol{\mu}^{-1}$, the inverse of the permeability, $\mathcal{C}^E$ reduces to $\mathbf{c}$, the mechanical stiffness and the remaining coefficient matrices are zero. Boundary conditions include zero magnetic potential on the air boundary, fixed and natural boundary conditions on the mechanical boundary, and continuity at material interfaces.

Simulation of the magnetic induction and strain response to a current density and body force begins from a known induction, strain, stress, and field condition (e.g., zero for all quantities.) The change in magnetic potential and displacement due to a change in current density and force are first calculated by solving (17). The change in induction is then calculated according to (13), the strain according to (16), and the stress and magnetic field according to (12). Finally, the total quantities are updated by adding the change to the initial quantities, the coefficient matrices are calculated with the new stress and field values, and the process is repeated for the next current density and force change.

SIMULATIONS

The boundary value problem (17) was solved for the 2-D case with a uniform compressive stress along the active material length, starting from an initial configuration of zero magnetic field, induction, and current density. Material properties consistent with Galfenol were used. The Galfenol sample is mechanically unconstrained. The $[010]$ crystal orientation is oriented along the Galfenol length directed up and the $[100]$ is along the Galfenol width directed to the right. The problem was solved numerically with the finite element method (FEM) using the PDE toolbox in Matlab. The geometry of the boundary value problem is shown in Figure 2. To analyze the effect of geometry and stress on the induction, magnetostriction, and domain volume fractions, simulations were performed with and without air gaps between the steel flux path and Galfenol and with and without stress applied to the Galfenol sample.

Figure 3 depicts measurable quantities that were calculated from the simulations. Figure 3(a) is the average magnetization over the cross-section of the Galfenol sample at its center plotted against the magnetic field located 3.2 mm from the surface at the rod center. Both quantities are for the $[010]$ direction. For an actual system, the magnetization would be calculated from the induction (measured with a pickup coil) and the magnetic field (measured with a Hall probe.) Both air gaps and stress tend to

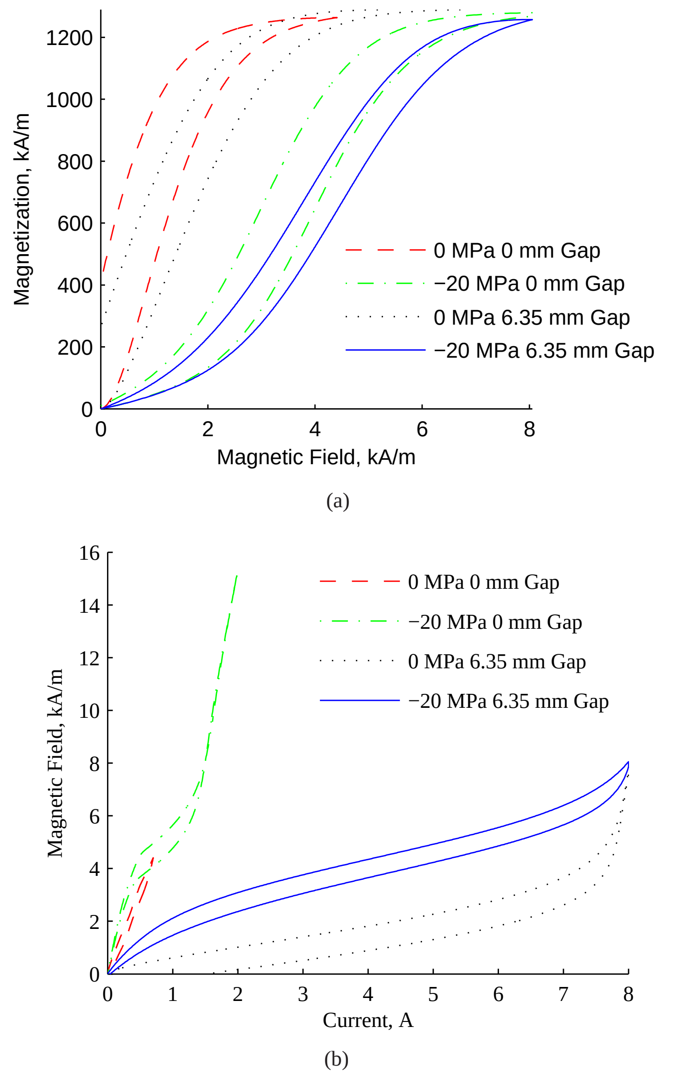

Figure 3. (a) MAGNETIZATION AND (b) FIELD SIMULATIONS FOR APPLIED CURRENT WITH AND WITHOUT STRESS AND AIR GAPS.

shear the induction versus field behavior. Stress impedes domain rotation and favors the $[100]$ and $[\bar{1}00]$ directions which are perpendicular to the stress. Air gaps result in flux-leakage which shears the curve. This causes a change in the current-field behavior as well (see Figure 3(b)) where more current is needed in the presence of air gaps. Stress changes the current-field curves because it changes the permeability of Galfenol. This nonlinear behavior as well as saturation result in a nonlinear current-field relationship. The relationship is hysteretic as a result of the hysteresis in Galfenol's constitutive behavior which gives rise to a hysteretic permeability.

The cause of the sheared field-magnetization behavior for simulations with air gaps is illustrated in Figure 4 which plots the FEM solution for the norm of the induction at saturation. Here, saturation is defined as the point where the average magnetization over the cross-section (Figure 3) reaches the material's saturation magnetization. The difference in permeability between the air, steel and Galfenol regions gives a nonuniform induction

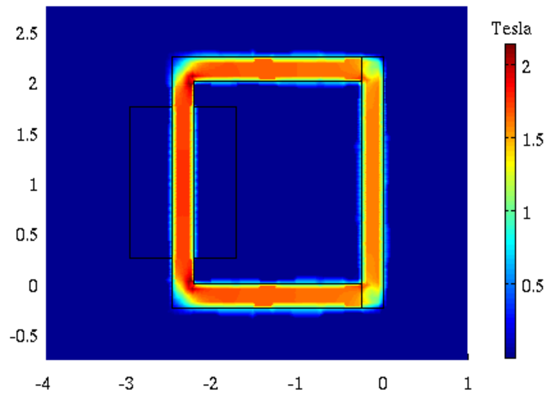

(a)

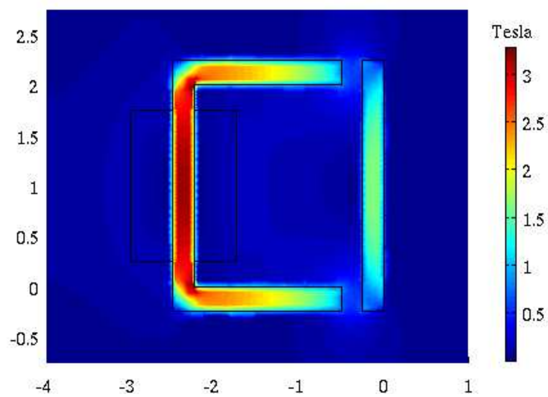

(b)

Figure 4. NORM OF INDUCTION AT SATURATION (a) WITHOUT AND (b) WITH AIR GAPS.

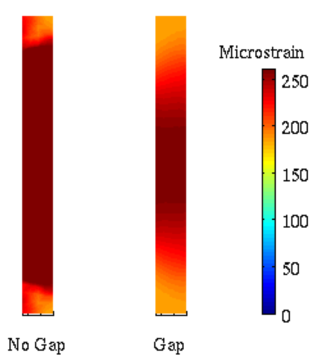

Figure 5. NORM OF STRAIN AT SATURATION WITH NO APPLIED STRESS.

from Gauss' law which can also be interpreted as the presence of a demagnetizing field which must be overcome by the current induced field. The nonuniformity for the case without air gaps (see Figure 4(a)) is much less because steel and Galfenol have similar permeability. This results in negligible demagnetizing fields and the Galfenol sample is easier to magnetize. Demagnetizing fields

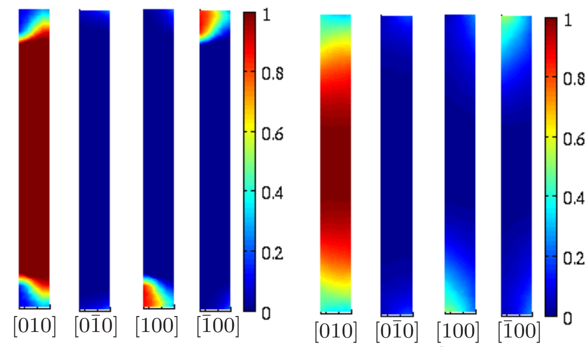

(a) (b)

Figure 6. DOMAIN VOLUME FRACTIONS IN GALFENOL AT SATURATION (a) WITHOUT AND (b) WITH AIR GAPS.

from Gauss' law also result in a nonuniform domain configuration. Although the modeling framework presented here does not encompass a microscopic description of domains including domain size, domain wall width and closure domains, the volume fraction of energetically favorable domain orientations in the material is calculated (see Figure 6.) Figure 6(a) shows a homogeneous domain distribution at saturation when there are no air gaps. The Galfenol consists almost entirely of $[010]$ oriented domains except for the ends where $[100]$ and $[\bar{1}00]$ domains are present to channel the flux through the steel return path. When air gaps are present (Figure 6(b)) the domain distribution is less homogeneous. Although saturation has been achieved at the center of the Galfenol sample, the rest of the material is not fully saturated as evidenced by the presence of domain orientations other than $[010]$. Because of the magnetomechanical coupling and nonuniformity in the magnetic state, the strain is nonuniform even though the stress is uniform (see Figure 5.)

Hysteresis in the domain volume fraction evolution modeled by Equation (11) results in a remanent induction and magnetostriction when the current is removed (see Figure 7.) Demagnetizing fields from air gaps and application of stress both tend to reduce the remanent induction. With no stress or air gaps, the remanent state has a significant fraction of domains in the $[010]$ orientation (see Figure 8(a)) resulting in a net induction at remanence following a magnetization cycle. Applied stress tends to favor the $[100]$ and $[\bar{1}00]$ directions equally (see Figure 8(b) and 8(d)) resulting in negligible net induction at remanence. Figure 8(c) shows a decrease in the volume fraction of $[010]$ oriented domains at remanence resulting in less induction. The norm of the magnetostriction exhibits behavior different from the norm of the induction because the magnetostriction of opposing directions (e.g., $[100]$ and $[\bar{1}00]$) does not cancel. Demagnetizing fields result in less domain alignment which yields less magnetostriction (see Figure 7(b).) However, application of stress results in a high degree of alignment in the $[100]$ and $[\bar{1}00]$ directions which have the same magnetostriction and thus a net magnetostriction or widening and simultaneous shortening of the Galfenol region occurs. Thus the remanent magnetostriction in the case of applied stress is not due to the magnetic hysteresis but rather to stress-induced domain alignment.

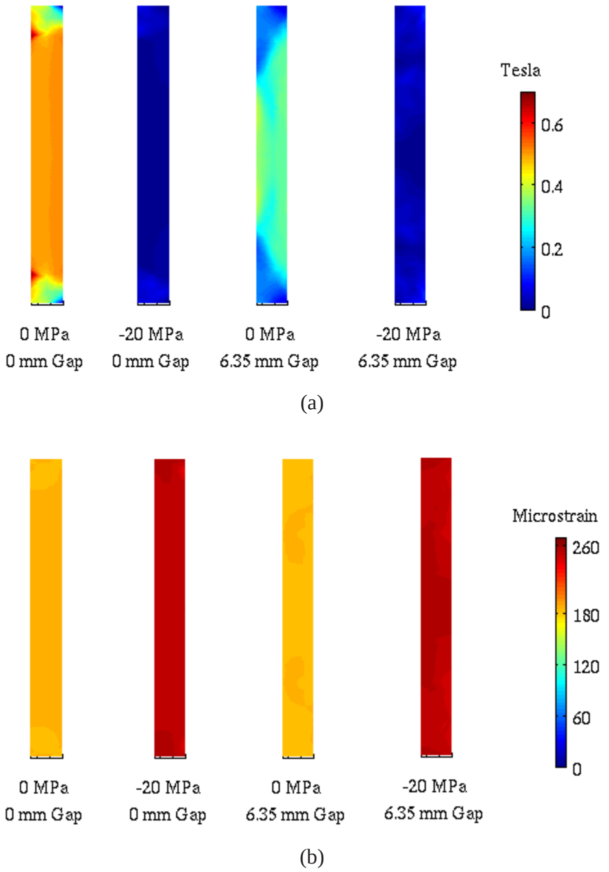

Figure 7. REMANENT (a) INDUCTION AND (b) STRAIN NORMS IN GALFENOL WITH AND WITHOUT STRESS AND AIR GAPS.

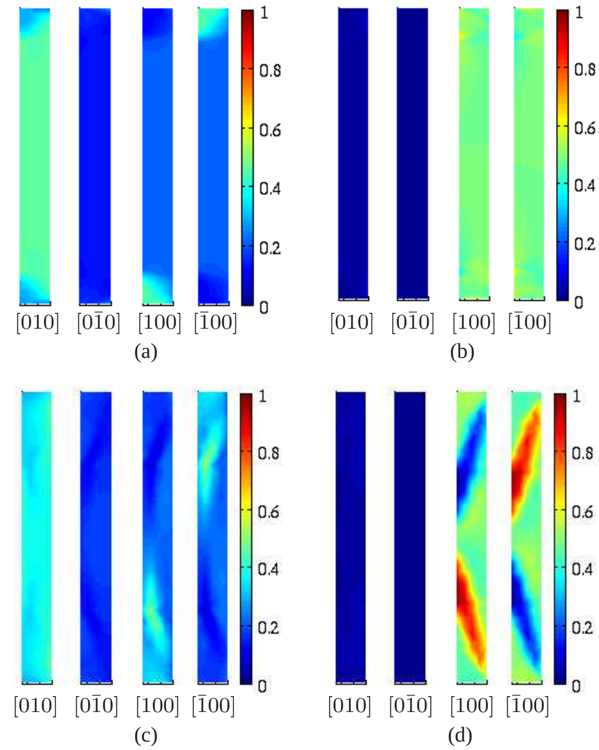

Figure 8. DOMAIN VOLUME FRACTIONS IN GALFENOL AT REMANENCE WITH (a) NO STRESS AND NO GAP (b) -20 MPa STRESS AND NO GAP (c) NO STRESS AND 6.35 mm GAPS (d) -20 MPa STRESS AND 6.35 mm GAPS.

CONCLUSION

A framework has been developed to model the 3-D coupled induction and strain response of cubic magnetostrictive materials to current and force. Thermodynamics was used to develop a computationally efficient constitutive model which includes the effects of intrinsic magnetomechanical coupling, magnetic anisotropy, saturation, and hysteresis. This constitutive model couples the magnetic and mechanical behavior of general magnetostrictive transducers which is described by Maxwell's equations and Newton's second law. The framework was implemented for a 2-D geometry with uniform stress to show the effects of geometry and stress on the induction and magnetostriction of Galfenol. Future work will include 3-D implementation and nonuniform stress due to material constraints and applied traction forces.

ACKNOWLEDGMENT

We wish to acknowledge the financial support by the Office of Naval Research, MURI grant #N000140610530.

REFERENCES

[1] Clark, A. E., Restorff, J. B., Wun-Fogle, M., Lograsso, T. A., and Schlagel, D. L., 2000. "Magnetostrictive properties of body-centered cubic Fe-Ga and Fe-Ga-Al alloys". *IEEE Trans. Magn.*, **36**(5), pp. 3238–3240.

[2] Oates, W. S., 2007. "Multiscale constitutive model development and finite element implementation for magnetostricti materials". In Proceedings of IMECE.

[3] Mudivarthi, C., Datta, S., Atulasimha, J., and Flatau, A. B., 2008. "A bidirectionally coupled magnetoelastic model and its validation using a Galfenol unimorph sensor". *Smart Materials and Structures*, **17**.

[4] Kiefer, B., Rosato, D., and Miehe, C., 2008. "Modeling and computational analysis of materials exhibiting intrinsic magnetomechanical coupling". In SPIE.

[5] Smith, R. C., Dapino, M. J., Braun, T. R., and Mortensen, A. P., 2005. "A homogenized energy framework for ferromagnetic hysteresis". *IEEE Trans. Magn.*, **42**(4), pp. 1747–1769.

[6] Armstrong, W. D., 1997. "Magnetization and magnetostriction processes". *Journal of Applied Physics*, **81**(5), pp. 23217–2326.

[7] Kittel, C., 1949. "Physical theory of ferromagnetic domains". *Review of Modern Physics*, **21**(4), Oct, pp. 541–583.

[8] ter Haar, D., 1995. *Elements of Statistical Mechanics*, 3rd ed. Butterworth-Heinemann, p. 158.

[9] Armstrong, W. D., 2003. "An incremental the-

ory of magneto-elastic hysteresis in pseudo-cubic ferro-magnetostrictive alloys". *Journal of Magnetism and Magnetic Materials*, **263**, p. 208.